Electrostatic interactions between graphene layers and their environment

J. Sabio,[1] C. Seoánez,[1] S. Fratini,[1,2] F. Guinea,[1] A. H. Castro Neto,[3] and F. Sols[4]
[1]*Instituto de Ciencia de Materiales de Madrid (CSIC), Sor Juana Inés de la Cruz 3, E-28049 Madrid, Spain*
[2]*Institut Néel-CNRS and Université Joseph Fourier, BP 166, F-38042 Grenoble, Cedex 9, France*
[3]*Department of Physics, Boston University, 590 Commonwealth Avenue, Boston, Massachusetts 02215, USA*
[4]*Departamento de Física de Materiales, Universidad Complutense de Madrid, E-28040 Madrid, Spain*
(Received 19 December 2007; revised manuscript received 4 March 2008; published 6 May 2008)

We analyze the electrostatic interactions between a single graphene layer and a SiO_2 substrate, and other materials which may exist in its environment. We obtain that the leading effects arise from the polar modes at the SiO_2 surface, and water molecules, which may form layers between the graphene sheet and the substrate. The strength of the interactions implies that graphene is pinned to the substrate at distances greater than a few lattice spacings. The implications for graphene nanoelectromechanical systems, and for the interaction between graphene and a scanning tunneling microscopy tip, are also considered.

DOI: 10.1103/PhysRevB.77.195409 PACS number(s): 81.05.Uw, 68.35.−p, 62.25.−g

I. INTRODUCTION

Graphene is a versatile two dimensional material whose singular electronic and mechanical properties show a great potential for applications in nanoelectronics.[1–3] Since free floating graphene is subject to crumpling,[4] the presence of a substrate, and the environment that comes with it, is fundamental for its stabilization. Hence, this environment will have a direct impact in the physical properties of graphene. Although the influence of the substrate and other elements of the surroundings has been taken into account in different ways in literature, the exact part that these are playing is not yet fully understood.

On the one hand, the differences observed between samples grown on different substrates constitute an open issue. Most experiments have been carried out in graphene samples deposited over SiO_2, or grown over SiC substrates,[5] and a better understanding of how graphene properties are expected to change would be worthy. On the other hand, there is the question of characterizing all the effects that a particular environment has on graphene electronic and structural properties.

Concerning electronic properties, it has been suggested that the low temperature mobility of the carriers is determined by scattering with charged impurities in the SiO_2 substrate,[6,7] and the effect of these charges can be significantly modified by the presence of water molecules.[8,9] Actually, the very polar modes of SiO_2 give a good description of the finite temperature corrections to the mobility.[10–12] Supporting this idea, recent experiments show that graphene suspended above the substrate has a higher mobility.[13,14]

Experiments also seem to reveal a very important role played by the substrate in the structural properties of graphene. Scanning tunneling microscopy (STM) measurements suggest that single layer graphene follows the corrugations of the SiO_2 substrate,[15,16] and experiments on graphene nanoelectromechanical systems (NEMSs) indicate that the substrate induces significant stresses in a few layer graphene samples.[17] Moreover, the interaction between graphene and the substrate determines the frequency of the out of plane (flexural) vibrations, which can influence the transport properties at finite temperatures.[18,19]

In order to shed light on the influence of the environment on the graphene properties, we analyze the characteristic energies of interaction with the substrate and other materials present in the experimental setup. This allows us to evaluate the relative importance of the different interactions in the binding and mechanical response of the graphene layer. We also provide estimates of quantities such as equilibrium distances, typical length scales of corrugations, and frequencies of vibration, which can be measured, in principle, in current experimental setups.

Throughout the paper, we concentrate on SiO_2, though results are easily generalized to other substrates. Particularly, we consider (i) the van der Waals forces between graphene and the metallic gate below the SiO_2 substrate, (ii) the electrostatic forces between the graphene layer and the polar modes of the substrate, (iii) the electrostatic forces between graphene and charged impurities, which may be present within the substrate, and (iv) the electrostatic forces between graphene and a water layer, which may lay between graphene and the substrate.[8,9] A sketch of the setup studied, and the different interaction mechanisms, is shown in Fig. 1. We will also mention the possibility of weak chemical bonds

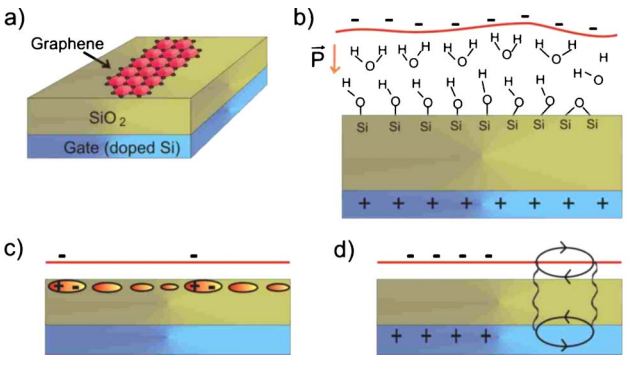

FIG. 1. (Color online) (a) Sketch of the system studied in the text. Interaction effects: (b) Interaction with water molecules attached to hydroxyl radicals at the substrate. (c) Interaction with polar modes at the surface of the substrate. (d) van der Waals interaction between the graphene sheet and the metallic gate.

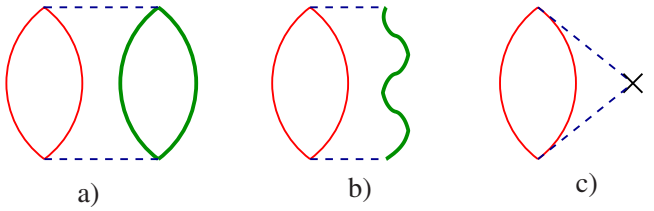

FIG. 2. (Color online) Lowest order diagrams, which contribute to the interaction between (a) graphene and a metal, (b) graphene and a polar dielectric, and (c) graphene and a static charge distribution. The thin red bubble stands for the graphene susceptibility. The thick green bubble represents the metallic susceptibility. The wavy green line stands for the propagator of a phonon mode in the dielectric. Crosses stand for static charge distributions, and dashed lines represent the electrostatic potential.

between the graphene layer and molecules adjacent to it,[20,21] although they will not be analyzed in detail. We do not consider a possible chemical modification of the graphene layer,[22,23] which would change its transport properties.

The general features of the electrostatic interactions to be studied are discussed in Sec. II. Then, we analyze, case by case, the different interactions between the graphene layer and the materials in its environment. Section III discusses the main implications for the structure and dynamics of graphene, with applications to graphene NEMSs and the interaction between graphene and a STM tip. Section IV presents the main highlights of our work.

II. ELECTROSTATIC INTERACTIONS BETWEEN A GRAPHENE LAYER AND ITS ENVIRONMENT

The electrons in the π and π^* bands of graphene are polarized by electromagnetic potentials arising from charges surrounding it. The van der Waals interactions between metallic systems, and metals and graphene can be expressed as integrals over the dynamic polarizability of both systems. Those, in turn, can be written in terms of the zero point energy of the plasmons.[24,25] The interaction between the graphene layer and a polarizable dielectric such as SiO_2 is also given by an integral of the polarizability of the graphene layer times the polarizability of the dielectric. The latter can be approximated by the propagator of the polar modes, which play a similar role to the plasmons in a metal. The interaction between the graphene and static charges of electric dipoles depends only on the static polarizability.[26]

We will calculate these interactions using second order perturbation theory, assuming a perfect graphene sheet so that the momentum parallel to it is conserved. The corresponding diagrams are given in Fig. 2. All interactions depend, to this order, linearly on the polarizability of the graphene layer. In ordinary metallic systems, the Coulomb interaction is qualitatively changed when screening by the graphene electrons is taken into account through a random phase approximation summation of diagrams. This is not the case for undoped graphene. There, the random phase approximation leads to a finite correction $\pi e^2/8\hbar v_F \sim 1$ to the dielectric constant, which does not significantly change the estimates obtained using second order perturbation theory.

The response function of a graphene layer at half filling is[27]

$$\chi_G(\vec{q},i\omega) = \frac{N_v N_s}{16\hbar} \frac{q^2}{\sqrt{v_F^2 q^2 + \omega^2}}, \tag{1}$$

where $N_s = N_v = 2$ are the valley and spin degeneracy. This expression is obtained assuming a linear dispersion around the K and K' points of the Brillouin zone. It is valid up to a cutoff in momentum $\Lambda \sim a^{-1}$ and energy $\omega_c \sim v_F \Lambda$, where a is the lattice spacing. Beyond this scale, the susceptibility has a more complex form, and it is influenced by the trigonal warping of the bands. The component of the electrostatic potential induced by a system at distance z from the graphene layer with momentum $\vec{q}$ is suppressed by a factor $e^{-|\vec{q}|z}$. Hence, the integrations over $\vec{q}$ can be restricted to the region $0 \leq q = |\vec{q}| \lesssim q_{\max} \sim z^{-1}$. The combination of a term proportional to $e^{-|\vec{q}|z}$ and scale invariant quantities such as the susceptibility in Eq. (1) leads to interaction energies, which depend as a power law on z. In general, we will consider only the leading term, neglecting higher order corrections.[28]

The calculation described above, which is valid for a single graphene layer at half filling, can be extended to other fillings and to systems with more than one layer. In all cases, the calculations are formally the same, and the interaction energies can be written as integrals over energies and momenta of the susceptibility of the system being considered, which replaces the susceptibility of a single layer, Eq. (1). The susceptibility of a doped single layer is well approximated by that of an undoped system, Eq. (1), for momenta such that $q \gtrsim k_F$.[29] Analogously, the susceptibilities of a stack of decoupled layers of graphene and multilayered graphene become similar for $q \gtrsim t_\perp/\hbar v_F$,[30] where $t_\perp$ is the hopping in the perpendicular direction. The susceptibility of a single undoped plane of graphene, Eq. (1), is an increasing function of q, so that the integrals are dominated by the region $q \sim q_{\max} \sim z^{-1}$. Hence, if $q_{\max} \gg k_F$ or $q_{\max} \gg t_\perp/\hbar v_F$, the interaction energies do not appreciably change from the estimates obtained for a single layer. The corrections can be obtained as an expansion in powers of either $k_F z$ or $(t_\perp z)/\hbar v_F$. Expression (1) can therefore be considered as the lowest order expansion in these parameters. For $z \sim 1$ nm, $t_\perp \sim 0.35$ eV and carrier densities such that $n \sim 10^{10}-10^{12}$ cm^{-2}, we obtain $k_F z \sim 10^{-2}-10^{-1}$ and $t_\perp/\hbar v_F \sim 10^{-2}-10^{-1}$. In the following, we will analyze mostly the interaction energies using the expression in Eq. (1) for the graphene polarizability.

A. Metallic gate

We describe the metallic gate as doped Si, separated from the graphene layer by a 300 nm thick slab of SiO_2 dielectric. For the Si doping and voltages applied, most of the charge in the Si gate is concentrated on a layer of about 10 nm thickness,[31] much narrower than the distance to the graphene sheet, so that the gate is effectively two dimensional. We describe the susceptibility of the gate as that of a dirty two dimensional electron gas, as follows:

$$\chi_{\text{gate}}(\vec{q},i\omega) = -\frac{dn}{d\mu}\frac{Dq^2}{Dq^2+|\omega|}, \tag{2}$$

where $D=v_{F_{\text{gate}}} l_{\text{gate}}$ is the diffusion coefficient of the electrons in the gate, $v_{F_{\text{gate}}}$ is the Fermi velocity, l_{gate} is the mean free path, and $dn/d\mu$ is the bare compressibility, given by the density of states at the Fermi level (see, for instance, Ref. 32).

The interaction between the graphene layer and the gate is given by

$$v_q(z) = \frac{2\pi e^2}{\epsilon}\frac{e^{-qz}}{q}, \tag{3}$$

being ϵ the static dielectric constant of the SiO_2 substrate.

The lowest order contribution to the energy in perturbation theory has the following form:

$$E^{(2)}_{\text{gate}} = -\hbar\sum_q \int_0^\infty \frac{d\omega}{2\pi} v_q^2(z)\chi_G(\vec{q},i\omega)\chi_{\text{gate}}(\vec{q},i\omega). \tag{4}$$

For future reference, note that we use the symbol E for energies per unit area, and $\mathcal{E}$ for total (integrated) energies. The resulting integrals can be analytically calculated in the limit $z_s \equiv D/4v_F \ll z$ as follows:

$$E^{(2)}_{\text{gate}} = -\frac{1}{12}\frac{dn}{d\mu}\frac{D}{v_F}\frac{e^4}{\epsilon^2}\frac{1}{(2z)^3}\left[\log\left(\frac{z}{z_s}\right)+\frac{1}{3}\right]. \tag{5}$$

The dependence on $z^{-3}\log(z/z_s)$ was obtained in Ref. 25.

We take, as representative parameters for the gate and the graphene layer, $D \approx 10^{-3}$ m^2/s, $v_F=10^6$ m/s, $z=300$ nm, $dn/d\mu \simeq g(E_F)=0.04$ eV^{-1} Å^{-2}, and $\epsilon=4$ for the SiO_2 substrate. These parameters lead to interaction energies of order $\sim 10^{-8}$ meV Å^{-2}.

B. Polar dielectric

The interaction between the graphene layer and the SiO_2 substrate can be expressed in terms of the electric fields induced by the surface polar modes of SiO_2.[33–36] The coupling can be written as

$$H_I = \sum_q M_q \rho_q (b_q + b^\dagger_{-q}), \tag{6}$$

where ρ_q is the electron density operator and $b^\dagger_q, b_q$ the creation and/or destruction operators for phonons, and $M_q^2 = (\hbar^2 v_F^2) g e^{-2qz}/(qa)$ is the interaction matrix element, with g a dimensionless coupling constant. In SiO_2, we have two dominant phonon modes at $\hbar\Omega_1=59$ meV and $\hbar\Omega_2=155$ meV, with $g_1=5.4\cdot 10^{-3}$ and $g_2=3.5\cdot 10^{-2}$, respectively.[11]

The lowest order contribution to the energy is given by

$$E^{(2)}_{\text{subs}} = \sum_i \sum_{\vec{q}} \int \frac{d\omega}{2\pi}\chi_G(\vec{q},i\omega)|M_q(z)|^2 D_i^{(0)}(\vec{q},i\omega), \tag{7}$$

where we have introduced the following free phonon propagators:

$$D_i^{(0)}(\vec{q},i\omega) = -\frac{2\Omega_i}{\omega^2+\Omega_i^2}. \tag{8}$$

The calculation can be again analytically carried out. In the limit $z \ll l_i \equiv v_F/\Omega_i$, we obtain

$$E^{(2)}_{\text{subs}} = -\sum_i \frac{\hbar v_F}{a}\frac{g_i}{(2z)^2}, \tag{9}$$

which gives a z^{-2} dependence on the distance. In the opposite limit $z \gg l_i$, which can be of interest in suspended graphene experiments, one obtains

$$E^{(2)}_{\text{subs}} = -\frac{\hbar v_F}{6a}\frac{1}{(2z)^3}\sum_i l_i g_i\left[\log\frac{l_i}{4z}+\frac{1}{3}\right]. \tag{10}$$

Let us give some numerical estimates for both expressions. In the case of graphene deposited over the substrate, we have $z \sim 1$ nm (see Ref. 2) and $l_i \ll z$, having interaction energies of order $E^{(2)}_{\text{subs}} \sim -4\times 10^{-1}$ meV Å^{-2}. For suspended graphene, $z \sim 300$ nm, and the energies are of order $E^{(2)}_{\text{subs}} \sim -10^{-8}$ meV Å^{-2}, i.e., of the same order than the contribution from the gate.

C. Charges within the substrate

In this case, the calculations are done considering that effectively all of the charge is concentrated close to the surface of the SiO_2 dielectric. The second order correction to the energy, averaged over the charge distribution, is

$$E^{(2)}_{ch} = -\sum_{\vec{q}} \chi_G(\vec{q},0) v_q^2(z) n_{\text{imp}}, \tag{11}$$

where we consider a Coulomb interaction v_q between graphene electrons and charges that is statically screened by the effective dielectric constant at the interface, $(\epsilon+1)/2$. Again, this contribution can be analytically carried out as follows:

$$E^{(2)}_{ch} = -\left(\frac{2e^2}{\epsilon+1}\right)^2 \frac{\pi n_{\text{imp}}}{2\hbar v_F}\frac{1}{2z}. \tag{12}$$

This interaction has a z^{-1} dependence, as the image potential in ordinary metals. In this case, however, this behavior arises from the combination of a vanishing density of states and lack of screening in graphene.

Reasonable values for the impurity concentration in graphene are in the range $n_{\text{imp}} \sim 10^{10}-10^{12}$ cm^{-2}.[6,7] Setting $z \sim 1$ nm, typical interaction energies are of the order $E_{ch} \sim -10^{-4}-10^{-2}$ meV Å^{-2}.

The present result is only valid for graphene samples close to the substrate. If the distance to the latter is larger than the typical distance between charges, $d_{\text{imp}} \sim \sqrt{n_{\text{imp}}} \sim 1-10$ nm, the electrons feel the net effect of the effective charge in the substrate. This is zero in average, as there should be a compensated number of positive and negative charges. However, if we consider a finite region of the substrate, fluctuations can locally give rise to a net effective charge. This can be estimated by replacing $N_{\text{imp}}=n_{\text{imp}}l^2 \to \sqrt{n_{\text{imp}}l^2}$ in the total energy $\mathcal{E}_{ch}=E^{(2)}_{ch}l^2$, where l is the lateral sample size.

D. Layer of water molecules

The properties of the SiO_2 surface are dominated, for thermally grown SiO_2 layers, by the presence of abundant silanol (SiOH) groups,[37] whose surface density is about 5×10^{14} cm^{-2}, unless extra steps like thermal annealing in high vacuum are taken during the fabrication process.[38–40] Silanol sites are active centers for water absorption, so that the SiO_2 surface becomes hydrated under normal conditions,[41] which is probably the case of most of the graphene samples produced by mechanical cleavage.[8] Moreover, several layers of water may cover the SiO_2 surface, lying between the oxide surface and the graphene samples after the graphene deposition. An analogous situation has been shown to happen in experiments with carbon nanotubes deposited on SiO_2.[42]

The water molecule has an electric dipole, $p_w = 6.2 \times 10^{-30}$ Cm $\approx 0.04e$ nm. Typical fields applied in present experimental setups are $\mathcal{E} \sim 0.1$ V nm^{-1}. The energy of a water dipole when it is aligned with this field is 4 meV ~ 50 K, so that, at low temperatures, it will be oriented along the field direction, perpendicular to the substrate and the graphene layer. For this reason, in the following, we assume that the water molecules are not charged, and their dipoles are aligned perpendicular to the substrate and the graphene layer. This arrangement can be considered as an upper bound to the interaction energy with a neutral water layer, as inhomogeneities and thermal fluctuations will induce deviations in the orientation of the dipoles, and will lower the interaction energy. Note, however, that for high applied electric fields, a charging of water molecules of the order $Q_{H_2O} \sim 0.1|e|$ has been reported.[42] The presence of these extra charges would considerably enhance the interaction between the graphene layer and the water molecules.

A water molecule, which is located at a distance z from the graphene layer, induces an electrostatic potential:

$$\Phi(\vec{q}, z, \vec{r}) = 2\pi p_w e^{-|\vec{q}|z} e^{i\vec{q}\vec{r}}, \tag{13}$$

where $\vec{r}$ is the two dimensional vector, which denotes the position of the molecule. This potential polarizes the graphene layer and gives rise to an interaction energy in a similar way to the static charges discussed in Sec. II C. The interaction energy can be written as

$$E^{(2)}_{\text{water}} = \sum_{\vec{r}_i} \sum_{\vec{r}_j} \int d^2\vec{q} (2\pi p_w e^{-|\vec{q}|z})^2 e^{i\vec{q}(\vec{r}_i - \vec{r}_j)} \chi(|\vec{q}|), \tag{14}$$

where the sum is over the positions of the water molecules. If these positions are uncorrelated, we have

$$\langle e^{i\vec{q}(\vec{r}_i - \vec{r}_j)} \rangle = \delta_{ij} \tag{15}$$

and Eq. (16) can be expressed as a sum over contributions from individual water molecules. Then, the lowest order contribution to the energy is

$$E^{(2)}_{\text{water}} = -(ep_w)^2 \frac{\pi}{6} \frac{n_w}{\hbar v_F} \frac{1}{(2z)^3}, \tag{16}$$

where n_w is the concentration of water molecules and the z^{-3} behavior arises from the dipolar nature of the interactions. For $z = 0.3$ nm, which is the approximate thickness of a water monolayer,[43,44] the interaction energy is $E^{(2)}_{\text{water}} \sim -12 n_w$ meV which, for a typical water concentration $n_w = 10^{15}$ cm^{-2}, yields $E^{(2)}_{\text{water}} \sim -1$ meV/Å^2.

The expression in Eq. (16) can be extended to a semi-infinite stack of water layers. For simplicity, we take a distance z between graphene and the uppermost layer of water molecules equal to the interlayer distance. In this case, we obtain

$$E^{(2)}_{\text{water}} = -(ep_w)^2 \frac{\pi}{6} \frac{n_w}{\hbar v_F} \frac{\zeta(3)}{(2z)^3}, \tag{17}$$

where $\zeta(3) \approx 1.202$ is Riemann's zeta function. The present result indicates that the first water layer is the one that mostly contributes to the binding.

If the water molecules form an ordered array, the average in Eq. (15) will show peaks when the vector $\vec{q}$ coincides with a reciprocal lattice vector of the water array, $\vec{G}_i$, and it will be suppressed otherwise. Then, the dependence on the distance of the interaction potential will be a sum of terms of the type $e^{-2|\vec{G}_i|z}$. Nevertheless, the disorder in the SiO_2 substrate experimentally observed[15,16] implies that the existence of an ordered array of water molecules is not likely.

E. van der Waals interaction between graphene layers

For comparison, in this section, we evaluate the van der Waals interaction between two graphene layers at the equilibrium distance. Using the same approximations as for the other contributions, we recover the result of Ref. 25,

$$E^{(2)}_{G-G} = -\frac{\pi e^4}{16\hbar v_F} \frac{1}{(2z)^3}. \tag{18}$$

For $z = 0.3$ nm, this expression gives an interaction energy of 30 meV Å^{-2}. This estimate is similar to other experimental and theoretical values of the graphene-graphene interaction,[45,46] and is at least 1 order of magnitude greater than the other contributions analyzed earlier.

III. ANALYSIS OF THE RESULTS

A. Comparison of the different interactions

Numerical estimates for the different interaction energies obtained for reasonable values of the parameters are listed in Table I. The present results show that the leading interactions are those between graphene and the polar modes of the SiO_2 substrate, and between graphene and a possible water layer on top of the substrate. Both effects are of similar order of magnitude in the present approximation, where we have assumed that the water molecules are aligned in the direction normal to the substrate.

The interactions for multilayer graphene samples can be obtained by adding the separate contributions from each layer. The different dependences on distance imply that the relative strength of the interactions in samples with many layers can change compared to the results of Table I. For instance, the effects of the polar substrate $\propto z^{-2}$ and of charged impurities $\propto z^{-1}$, which are of longer range, sum up

TABLE I. Interaction energy per unit area for the mechanisms studied in this paper. For the numerical estimates, we have used typical concentrations of $10^{10}-10^{12}$ cm^{-2} charged impurities and 10^{15} cm^{-2} water molecules.

	Distance (nm)	Dependence on distance	Energy (meV Å^{-2})
Gate	300	$z^{-3}\log(z/z_s)$	10^{-8}
Charged impurities	1	z^{-1}	$10^{-4}-10^{-2}$
SiO_2 substrate ($z \ll l_i$)	1	z^{-2}	0.4
SiO_2 substrate ($z \gg l_i$)	300	$z^{-3}\log(4z/l_i)$	10^{-8}
Water molecules	0.3	z^{-3}	1
Graphene	0.3	z^{-3}	30

more effectively than the binding effect of water: The z^{-3} decay of the graphene-water interaction suggests that only the first graphene layer is affected by the presence of water on the substrate. For the same reason, the presence of several layers of aligned water molecules should not increase the binding, as only the closest layer effectively contributes to the interaction energy. On the other hand, the binding effect of water could be enhanced if the molecules were allowed to freely rotate, therefore approaching the high polarizability of liquid water,[8] or if they were partly ionized by the applied field,[42] leading to additional charges similar to the Coulomb impurities present in the SiO_2 substrate.

It should be noted that we have considered here only long-range electrostatic interactions, for which reliable expressions can be obtained, in terms of well understood material parameters, such as molecular polarizability, electric dipoles, or surface modes. Still, there is a significant uncertainty in some parameters, such as the distance of the relevant charges to the graphene layer and the concentration of charged impurities and water molecules. We have not analyzed the possible formation of chemical bonds between the carbon atoms and the water or silanol groups at the SiO_2 surface. Calculations based on the local density functional approximation[20,21] suggest that individual molecules can (weakly) bind to a graphene layer with energies of 10–50 meV, although it is unclear how these estimates are changed when the molecules interact at the same time with the graphene layer and the substrate.

B. Corrugation of the graphene layer induced by the substrate

The attractive forces calculated in Sec. II imply that graphene is bound to the SiO_2 substrate, as observed in experiments. Our previous analysis does not include the short-range repulsive forces, which determine the equilibrium distance. We assume that the total energy near the surface is the sum of the terms analyzed above, which have a power law dependence on the distance, and a repulsive term, $E_{\rm rep}(z) = \epsilon_{\rm rep}(z_0^n/z^n)$, which also decays as a power law at long distances, with z_0 an undetermined length scale. For simplicity, we assume that the leading attractive term is due to the presence of a water layer, which behaves as $E_{\rm water} = -\epsilon_w(z_0^3/z^3)$. The total energy per unit area is thus

$$E(z) = \epsilon_{\rm rep}\frac{z_0^n}{z^n} - \epsilon_w\frac{z_0^3}{z^3}. \tag{19}$$

At the equilibrium distance, $z_{\rm eq}$, we have

$$\frac{\epsilon_{\rm rep}}{\epsilon_w} = \frac{3}{n}\left(\frac{z_{\rm eq}}{z_0}\right)^{n-3}, \tag{20}$$

so that

$$\begin{aligned} E''(z_{\rm eq}) &= \frac{1}{z_{\rm eq}^2}\left[n(n+1)\epsilon_{\rm rep}\left(\frac{z_0}{z_{\rm eq}}\right)^n - 12\epsilon_w\left(\frac{z_0}{z_{\rm eq}}\right)^3\right] \\ &= 3(n-3)\frac{\epsilon_w}{z_{\rm eq}^2}\left(\frac{z_0}{z_{\rm eq}}\right)^3 \\ &= 3(n-3)\frac{E_{\rm water}(z_{\rm eq})}{z_{\rm eq}^2}. \end{aligned} \tag{21}$$

Hence, the order of magnitude of the pinning potential induced by the environment on the out of plane modes of graphene is given by $K \propto E_{\rm water}(z_{eq})/z_{eq}^2 \sim 10^{-2}-10^{-1}$ meV Å^{-4}. Defining the out of plane displacement as $h(\vec{r})$, the energy stored in a corrugated graphene layer is

$$\epsilon \approx 12\int d^2\vec{r}[\kappa(\Delta h)^2 + Kh^2], \tag{22}$$

where $\kappa \approx 1$ eV is the bending rigidity of graphene.[47,48] For modulations $h(\vec{r})$ defined by a length scale l, the bending energy dominates if $l \ll l^* = (\kappa/K)^{1/4}$, while the graphene layer can be considered rigidly pinned to the substrate if $l \gg l^*$. Using our previous estimates, we find $l^* \sim 10$ Å, so that the graphene layer should closely follow the corrugations of the substrate.

The pinning by the substrate implies that the dispersion of the flexural modes becomes

$$\omega_k = \sqrt{\frac{K}{\rho} + \frac{\kappa k^4}{\rho}}, \tag{23}$$

where ρ is the mass density of the graphene layer. At long wavelengths, $\lim_{k\to 0}\omega_k = \omega_0 \sim 10^{-4}-10^{-3}$ meV $\sim 10^{-3}-10^{-2}$ K.

The estimates obtained above also allow us to analyze the bending of graphene NEMSs due to the interaction with the material below, at distance d.[17,49] We assume that the lateral dimension of the graphene cantilever is l, and the maximum displacement of the graphene layer from a flat position is h. A sketch of the graphene cantilever is shown in Fig. 3. We consider the force induced by charged impurities in the substrate below the cantilever, as this is the contribution which decays more slowly with the distance to the graphene layer (cf. Table I). If the distance of the cantilever to the substrate is d, and supposing $d \gg h$, the gain in energy due to the deformation of the graphene layer is $\Delta\mathcal{E} \sim \epsilon_{ch} l z_0 h/\sqrt{n_{\rm imp}} d^2$. We have again defined z_0 and ϵ_{ch} by rescaling $E_{ch}(d) = \epsilon_{ch} z_0/d$, with $z_0 \sim 1$ nm and $\epsilon_{ch} \sim 10^{-4}-10^{-2}$ meV Å^{-2} depending on the density of impurities. The factor $l/\sqrt{n_{\rm imp}}$ is included, as already mentioned at the end of Sec. II C, to take into account the effect of having an overall neutral dis-

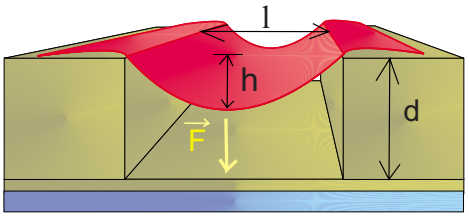

FIG. 3. (Color online) Sketch of the deformation of a nanoelectromechanical device studied in the text.

tribution of charge in the substrate. This energy should compensate the elastic response to the deformation, $\Delta\mathcal{E}_{el} \sim \kappa h^2/l^2$, leading to an equilibrium value:

$$h \sim \frac{\epsilon_{ch} z_0}{2\kappa} \frac{l^3}{d^2\sqrt{n_{\text{imp}}}}. \tag{24}$$

Reminding the dependence of ε_{ch} on the density of impurities, Eq. (24) results in a behavior $h \propto \sqrt{n_{\text{imp}}}$. For structures such that $d \sim 300$ nm, one finds that the suspended graphene sheet significantly deforms (i.e., h becomes comparable with d) for lengths greater than a few μm.

In the case of very pure substrates (i.e., neglecting the presence of charged impurities), the attractive force that bends the graphene sheet would be determined by the next corrections to the energy, which decay as z^{-3}. Rewriting $E^{(2)} \sim -(\epsilon_w + \epsilon_{ph} + \epsilon_G)(z_0/z)^3$ with $\epsilon_{ph} \simeq \epsilon_G \sim 0.1$ meV/Å^2 and $\epsilon_w \sim 0.01$ meV/Å^2, we see that those interactions are dominated by the coupling to the gate and to the polar modes, which are of comparable magnitude. A calculation similar to the one presented above would yield deformations of the order of $h \sim 1$ Å $\times (l/d)^4$, resulting even in these cases to unstable graphene sheets for lengths greater than a few μm.

C. Interaction with a metallic tip in a scanning tunneling microscopy experiment

It is known that STM tips on graphite surfaces sometimes deform the surface graphene layer,[50,51] and the understanding of these deformations can be of interest for current research on graphene.[15,16,52] The analysis of the electrostatic interactions between a graphene layer and its environment allows us to estimate possible deformations induced by an STM tip. We analyze the setup sketched in the inset of Fig. 4. The tip has a lateral dimension l and it is located at a distance d from a graphene layer. This graphene layer interacts with an underlying substrate, and a voltage V is applied between the graphene layer and the tip. We consider three interactions:

(i) An attraction between the tip and the graphene layer, which tends to deform the graphene, in the way shown in Fig. 4. We assume that this energy is purely electrostatic. A simple estimate can be obtained by describing the setup as a capacitor where the area of the plates is l^2, the distance between the plates is d, and the applied voltage is V. The interaction energy is of the following order:

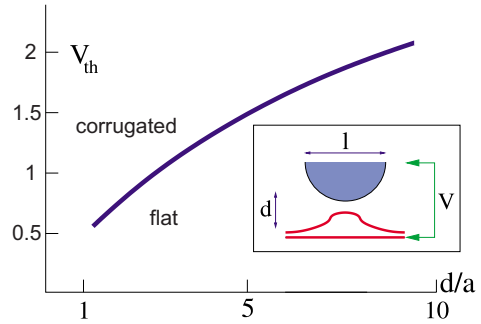

FIG. 4. (Color online) Estimate of the threshold voltage as a function of graphene-tip separation needed to detach a graphene layer from the substrate. The inset shows a sketch of the geometry considered in the text.

$$\mathcal{E}_{G\text{-tip}} \approx \frac{V^2 l^2}{8\pi e^2 d}, \tag{25}$$

where we define V in energy units.

(ii) The pinning of the graphene layer to the substrate. This contribution opposes the deformation of the layer. We write it as

$$\mathcal{E}_{\text{pin}} \approx \epsilon_{\text{pin}} l^2, \tag{26}$$

where ϵ_{pin} is the pinning energy per unit area. As typical values, we will use 1 meV/Å^2 for graphene on a water layer, and 30 meV/Å^2 for graphene interacting with another graphene layer, as in graphite.

(iii) The rigidity of the layer against flexural deformations. This term tends to keep the layer flat. The deformed region is likely to be (at least) as large as the size of the STM tip. As a result, an upper bound to the energy stored in a deformation is

$$\mathcal{E}_{el} \approx \kappa \frac{d^2}{l^2}. \tag{27}$$

The graphene layer will be deformed when

$$\mathcal{E}_{G\text{-tip}} \gtrsim \mathcal{E}_{\text{pin}} + \mathcal{E}_{el}. \tag{28}$$

Note that the approximations involved in obtaining the various terms are valid only if $d \gtrsim a$.

We consider a situation where ϵ_{pin}, k, and l are fixed. Equation (28) implies that the layer is deformed if the voltage exceeds a threshold as follows:

$$V \gtrsim V_{\text{th}}(d) \approx \sqrt{8\pi\left(\frac{\kappa e^2 d^3}{l^4} + \epsilon_{\text{pin}} e^2 d\right)}. \tag{29}$$

Assuming $l \sim 10a$ and $d \sim a$, we see that the dominant contribution comes from the pinning term (26). Hence, in the physically relevant range $a \lesssim d \ll l$, we can write

$$V_{\text{th}}(d) \approx \sqrt{8\pi\epsilon_{\text{pin}} e^2 d}, \tag{30}$$

independent of the tip size. The threshold values for graphene on SiO_2 are of about 0.5–2 V for $d \sim 1$–10 Å, as schematically shown in Fig. 4.

IV. CONCLUSIONS

We have analyzed the electrostatic interactions between a graphene layer and the polarizable materials which may be present in its environment, for samples deposited on SiO_2. The strength of these interactions can be obtained in terms of a few well understood microscopic parameters, and they have a simple dependence on the distance between the graphene layer and the system, which induces the electrostatic field. The analysis presented here should give reliable estimates of the order of magnitude of the different binding energies, and of their relative strength. We have not considered the possible formation of chemical bonds, which may alter the results when the distances between the carbon atoms in the graphene layer and the surrounding materials is sufficiently small.

We find that the leading effects arise from the polar modes of the SiO_2 substrate, and water which may form layers on top of it. A summary of the main results is presented in Table I. The interaction energies with systems with N layers can be obtained, to a first approximation, by adding the contributions from each layer. The estimated magnitude of the interactions suggests that a single graphene layer is pinned to the substrate on length scales greater than a few lattice spacings, ~ 10 Å. The electrostatic binding modifies the long wavelength, out of plane flexural modes, which acquire a finite frequency, $\omega_0 \sim 10^{-4} - 10^{-3}$ meV. The long-range forces considered here can also induce large deformations in graphene NEMSs. Besides, we have analyzed the possibility of deformations of the graphene layer by an STM tip. We find that a voltage drop of 0.5–2 V between the tip and the sample at distances 1–10 Å is sufficient to deform the graphene layer.

ACKNOWLEDGMENTS

This work was supported by MEC (Spain) through Grant No. FIS2005-05478-C02-01, the Comunidad de Madrid through the program CITECNOMIK, CM2006-S-0505-ESP-0337, the European Union Contract No. 12881 (NEST) (J.S., C.S., S.F., and F.G.), MEC through Grants No. FIS2004-05120 and No. FIS2007-65723, and EU Marie Curie RTN Programme No. MRTN-CT-2003-504574 (F.S. and J.S.). J.S. acknowledges the I3P Program from CSIC, and C.S. the FPU Program from MEC, for funding. We are thankful to A. Bachtold and A. K. Geim for many helpful insights into the relevance of water for current experiments, to S. Vieira for useful information on the interaction between graphene and STM tips, and to A. A. Balandin for a clarifying remark on our results for suspended graphene.

[1] K. S. Novoselov, D. Jiang, F. Schedin, T. J. Booth, V. V. Khotkevich, S. V. Morozov, and A. K. Geim, Proc. Natl. Acad. Sci. U.S.A. **102**, 10451 (2005).
[2] A. K. Geim and K. S. Novoselov, Nat. Mater. **6**, 183 (2007).
[3] A. H. Castro Neto, F. Guinea, N. M. R. Peres, K. S. Novoselov, and A. K. Geim, arXiv:0709.1163, Rev. Mod. Phys. (to be published).
[4] D. Nelson, D. Piran, and S. Weinberg, *Statistical Mechanics of Membranes and Surfaces* (World Scientific, Singapore, 2004).
[5] C. Berger *et al.*, J. Phys. Chem. B **108**, 19912 (2004).
[6] K. Nomura and A. H. MacDonald, Phys. Rev. Lett. **98**, 076602 (2007).
[7] S. Adam, E. H. Hwang, V. M. Galitski, and S. Das Sarma, Proc. Natl. Acad. Sci. U.S.A. **104**, 18392 (2007).
[8] F. Schedin, A. K. Geim, S. V. Morozov, D. Jiang, E. H. Hill, P. Blake, and K. S. Novoselov, Nat. Mater. **6**, 652 (2007).
[9] J. Moser, A. Verdaguer, D. Jiménez, A. Barreiro, and A. Bachtold, Appl. Phys. Lett. **92**, 123507 (2008).
[10] A. G. Petrov and S. V. Rotkin, JETP Lett. **84**, 156 (2006).
[11] S. Fratini and F. Guinea, arXiv:0711.1303, Phys. Rev. B (to be published).
[12] J. H. Chen, C. Jang, S. Xiao, M. Ishigami, and M. S. Fuhrer, Nat. Nanotechnol. **3**, 206 (2008).
[13] K. I. Bolotin, K. J. Sikes, Z. Jiang, G. Fudenberg, J. Hone, P. Kim, and H. L. Stormer, arXiv:0802.2389 (unpublished).
[14] X. Du, I. Skachko, A. Barker, and E. Y. Andrei, arXiv:0802.2933 (unpublished).
[15] M. Ishigami, J. Chen, W. Cullen, M. Fuhrer, and E. Williams, Nano Lett. **7**, 1643 (2007).
[16] E. Stolyarova, K. T. Rim, S. Ryu, J. Maultzsch, P. Kim, L. E. Brus, T. F. Heinz, M. S. Hybertsen, and G. W. Flynn, Proc. Natl. Acad. Sci. U.S.A. **104**, 9209 (2007).
[17] J. S. Bunch, A. M. van der Zande, S. S. Verbridge, I. W. Frank, D. M. Tanenbaum, J. M. Parpia, H. G. Craighead, and P. L. McEuen, Science **315**, 490 (2007).
[18] M. I. Katsnelson and A. K. Geim, Philos. Trans. R. Soc. London, Ser. A **366**, 195 (2008).
[19] S. Morozov, K. S. Novoselov, M. I. Katsnelson, F. Schedin, D. Elias, J. A. Jaszczak, and A. K. Geim, Phys. Rev. Lett. **100**, 016602 (2008).
[20] O. Leenaerts, B. Partoens, and F. M. Peeters, Phys. Rev. B **77**, 125416 (2008).
[21] T. O. Wehling, K. S. Novoselov, S. V. Morozov, E. E. Vdovin, M. I. Katsnelson, A. K. Geim, and A. I. Lichtenstein, Nano. Lett. **8**, 173 (2008).
[22] T. J. Echtermeyer, M. C. Lemme, M. Baus, B. N. Szafranek, A. K. Geim, and H. Kurz, arXiv:0712.2026 (unpublished).
[23] X. Wu, M. Sprinkle, L. X. F. Ming, C. Berger, and W. A. de Heer, arXiv:0712.0820 (unpublished).
[24] S. L. Tan and P. W. Anderson, Chem. Phys. Lett. **97**, 23 (1983).
[25] J. F. Dobson, A. White, and A. Rubio, Phys. Rev. Lett. **96**, 073201 (2006).
[26] For a metal, this interaction can be written as the interaction between the charge distribution and its image.
[27] J. González, F. Guinea, and M. A. H. Vozmediano, Nucl. Phys. B **424**, 596 (1994).
[28] Note that a polar dielectric introduces new length scales, $l_i = v_F/\Omega_i$, associated with the frequencies of its normal modes, Ω_i; see Sec. II B.
[29] B. Wunsch, T. Stauber, F. Sols, and F. Guinea, New J. Phys. **8**, 318 (2006).
[30] F. Guinea, Phys. Rev. B **75**, 235433 (2007).

[31] S. Sze, *Physics of Semiconductor Devices* (Wiley-Interscience, New York, 1981).
[32] F. Guinea, R. A. Jalabert, and F. Sols, Phys. Rev. B **70**, 085310 (2004).
[33] J. Sak, Phys. Rev. B **6**, 3981 (1972).
[34] S. Q. Wang and G. D. Mahan, Phys. Rev. B **6**, 4517 (1972).
[35] N. Mori and T. Ando, Phys. Rev. B **40**, 6175 (1989).
[36] I. N. Hulea, S. Fratini, H. Xie, C. L. Mulder, N. N. Iossad, G. Rastelli, S. Ciuchi, and A. F. Morpurgo, Nat. Mater. **5**, 982 (2006).
[37] B. Morrow, and A. McFarlan, J. Non-Cryst. Solids **120**, 61 (1990).
[38] O. Sneh and S. George, J. Phys. Chem. **99**, 4639 (1995).
[39] Y. Dong, S. Pappu, and Z. Xu, Anal. Chem. **70**, 4730 (1998).
[40] J. Nawrocki, J. Chromatogr. A **779**, 29 (1997).
[41] A. M. Botelho do Rego and L. F. Vieira Ferreira, *Handbook of Surfaces and Interfaces of Materials* (Academic, New York, 2001), Vol. 2, p. 275.
[42] W. Kim, A. Javey, O. Vermesh, Q. Wang, Y. Li, and H. Dai, Nano Lett. **3**, 193 (2003).
[43] M. Antognozzi, A. Humphris, and M. Miles, Appl. Phys. Lett. **78**, 300 (2001).
[44] A. Opitz, M. Scherge, S.-U. Ahmed, and J. Schaefer, J. Appl. Phys. **101**, 064310 (2007).
[45] L. X. Benedict, N. G. Chopra, M. L. Cohen, A. Zettl, S. G. Louie, and V. H. Crespi, Chem. Phys. Lett. **286**, 490 (1998).
[46] M. Hasegawa, K. Nishidate, and H. Iyetomi, Phys. Rev. B **76**, 115424 (2007).
[47] E.-A. Kim and A. H. Castro Neto, arXiv:cond-mat/0702562 (unpublished).
[48] E. Mariani and F. von Oppen, Phys. Rev. Lett. **100**, 076801 (2008).
[49] C. Seoánez, F. Guinea, and A. H. Castro Neto, Phys. Rev. B **76**, 125427 (2007).
[50] J. P. Batra, N. García, H. Rohrer, H. Salemink, E. Stoll, and S. Ciraci, Surf. Sci. **181**, 126 (1987).
[51] M. Salmeron, D. F. Ogletree, C. Ocal, H. C. Wang, G. Neubauer, W. Kolbe, and G. Meyers, J. Vac. Sci. Technol. B **9**, 1347 (1991).
[52] G. Li and E. Y. Andrei, Nat. Phys. **3**, 623 (2007).